JOURNAL OF MATERIALS SCIENCE **35** (2000) 477–486

Functionally graded materials by electrochemical processing and infiltration: application to tungsten/copper composites

R. JEDAMZIK, A. NEUBRAND, J. RÖDEL
TU Darmstadt, Petersenstr. 23, D-64287 Darmstadt, Germany
E-mail: neubrand@ceramics.tu-darmstadt.de

A novel processing route is presented that is capable of manufacturing composites with continuous gradients in chemical composition. This route is based on an electrochemical gradation and subsequent infiltration of porous preforms and allows production of a variety of functionally graded materials and geometries. The method allows flexible adjustment of the retained gradients by adjusting experimental parameters. Relevant electrode kinetics are cast into a macroscopic model which provides a predictive capacity for the gradients obtained. Tungsten/copper gradient materials with different gradation profiles were produced and a comparison of the observed with the calculated gradients was carried out.

1. Introduction

Functionally graded materials are materials with a smooth gradient in one or more properties which is essential for their function. The property gradient is usually caused by a gradient in chemical composition or microstructure. Although these materials are widespread in nature—graded structures are found in the culms of bamboo and barley and many other plants—it was only in 1984 that the concept of functionally graded materials (FGM's) has been developed by Niino and co-workers who were searching for materials capable of withstanding the high heat fluxes occurring during the re-entry of space vehicles. Since then, it has been recognised that the concept of a property gradation can be useful in many applications where one component has to fulfil contrasting requirements in different positions and a joint is inappropriate. Examples are hard materials, biomaterials, thermal barriers, materials for energy conversion or ultrasonic transducers. Increased performance, however, has mostly been hampered by increased manufacturing costs. Widespread transferral into the marketplace therefore requires an extensive search for cheap, reproducible and reliable manufacturing methods for FGM's.

A variety of methods to produce gradient materials has been reported in the literature. An overview of these processing techniques can be found in the literature [1, 2]. The most popular method is powder processing, where different mixtures of powders are stacked [3], slip cast [4] or pressure filtrated [5]. Gradient materials are also produced by thermal or plasma spraying [6].

Although suitable gradients can be produced by all of these methods, processing is often expensive and not suitable for stepless gradients. In the present work a novel electrochemical method for the production of stepless FGM's is presented with an application to graded tungsten/copper composites. The method is based on the electrochemical modification of porous preforms and subsequent infiltration steps. It is able to produce a large variety of graded composites, e.g. metal/metal- or metal/ceramic-FGM's. By adjusting experimental parameters like current density, electrolyte type and conductivity or electrical charge passed through the material, different gradation profiles can be produced. Graded bodies with different shape and symmetry can be fabricated by using suitably shaped electrodes.

Tungsten/copper composites show an excellent resistance to electric discharges and are therefore used as contact materials in high power switches and plasma-facing components. Their high thermal conductivity makes them attractive as heat sink materials where pure copper is not suitable, for example for cooling electronic substrates where tungsten/copper composites with different compositions can closely match the thermal expansion coefficient of almost any ceramic substrate. Gradation of tungsten/copper composites can have a number of advantages, the most important being the ease with which the copper side of the graded composite can be bonded to other materials. Gradation may be particularly useful in applications where the bond is exposed to repeated thermal shock leading to accumulation of plastic strains and fracture at the bonded interface [7]. Graded W/Cu composites have also potential as heat sinks in fusion reactors [8].

The first graded tungsten/copper composites have been manufactured by Takahashi *et al.* [9]. They produced tungsten preforms with graded porosity by stacking, sintering and capsule-free hot isostatic pressing of tungsten powders with different particle size and

infiltration of the resulting porous bodies. Dense bodies with a stepped gradient from 60 to 100% tungsten content could be produced. However, different shrinkage of the tungsten layers lead to strong deformation during sintering which could be only avoided by precompacting the different layers separately to different initial porosity. Therefore, efforts have been made recently to produce W/Cu FGM's directly by layering and sintering W and Cu powder mixtures of variable composition [10]. It appears, however, that densification of powder compacts with gradients from 0 to 100% copper content is difficult due to the very different sintering behaviour of W and Cu powders. Plasma spraying of W/Cu powder mixtures of variable composition has also been used for the production of W/Cu FGM's [11]. It allows production of graded composites with pure copper on one side and pure tungsten on the other side, but the plasma sprayed W/Cu FGM's have significant residual porosity affecting their performance in many applications. In the present paper the aforementioned novel production route is employed to produce dense W/Cu FGM's at reasonable cost.

2. General description of process

The process is based on the position dependent electrochemical reaction of porous preforms. After introducing a porosity gradient into the porous precursor material a variety of further processing steps can be carried out. They are illustrated in Fig. 1.

A starting material "O" with open porosity is needed which can be electrochemically dissolved or deposited. After the electrochemical treatment a product A with a gradient in porosity is retained. One can either use this porosity gradient material as such or infiltrate its open pores with the melt or liquid precursor of a second material (route I). The result will be a functionally graded material (Product B) where the more refractory phase is an electrical conductor, with the FGM being either a metal/metal, metal/polymer or carbide/metal composite. If the more refractory phase of the composite is an electrical insulator (as is the case with most oxide ceramics) a different route (II) has to be employed. This route uses a sacrificial preform from a starting material "O", which can be burnt, evaporated or dissolved (e.g. carbon). After the electrochemical gradation this material is infiltrated with a ceramic slip. In the next processing step the starting material is removed (e.g. by burn out) and the skeletal ceramic green body is sintered. The resulting ceramic body has a gradient in porosity which is reciprocal to that of the carbon preform. One can either use this ceramic graded in porosity (product C) directly (e.g. as a graded ceramic filter) or infiltrate it

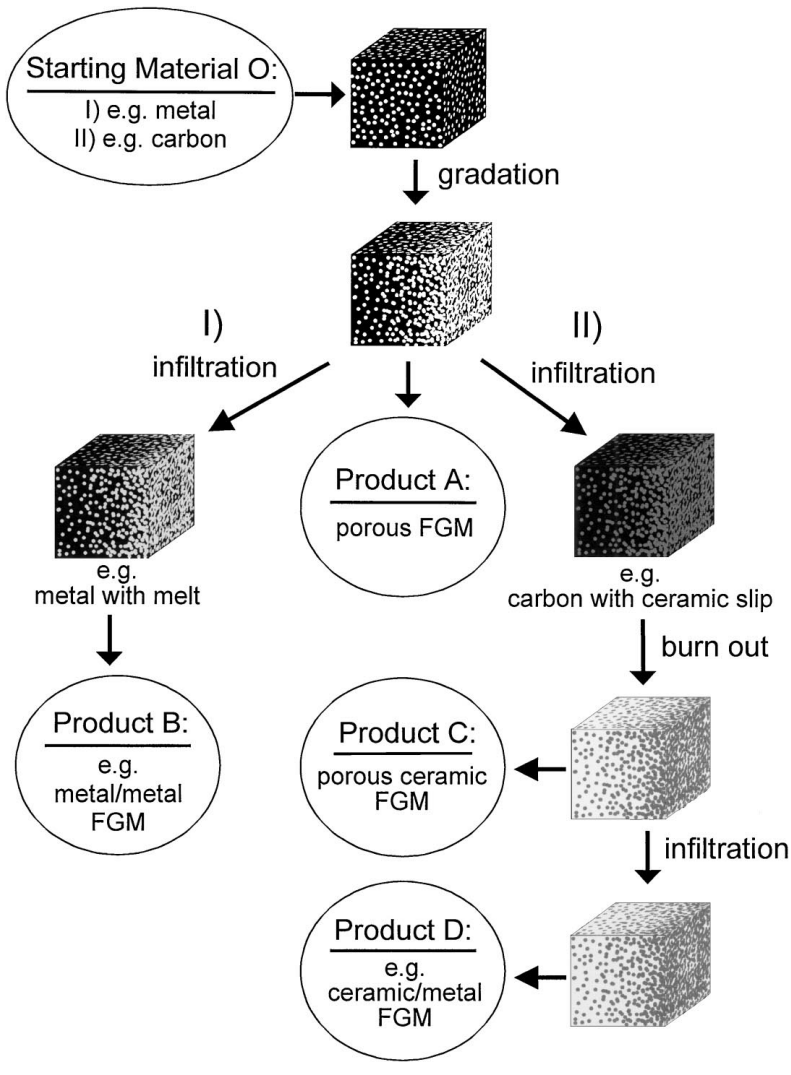

Figure 1 Overview of the different processing sequences possible.

with a liquid phase, which can be solidified. The product (D) can be a metal/ceramic or polymer/ceramic gradient material. Hence, by using the different processing routes a wide variety of FGM's is accessible.

3. Theory of electrochemical gradation

In contrast to dense electrodes the reaction in a porous electrode is not restricted to the external surface. If the electrolyte fills the pore space, the electrode reaction will also take place inside the pores. An electrode reaction accompanied by deposition or dissolution of electrode material will alter the porosity of the electrode. As the potentials of the different phases are usually position dependent, the electrochemical reaction will have different rates at different positions inside the porous electrode. In order to control the profile of the porosity gradient in an electrochemical gradation experiment a fundamental understanding of the potential distribution and the physicochemical processes taking place in the porous system is essential. In the following section a macroscopic model which describes the porous electrode as a homogeneous mixture of two phases will be developed. It neglects the precise shape of individual pores which is reasonable as long as the pore dimensions are much smaller than the electrode itself.

3.1. Theoretical background

Electrochemical gradation of porous preforms is based on the electrochemical reaction taking place in a pore system when the preform is connected as anode or cathode of an electrolysis cell. In the following section, let us consider a system undergoing anodic dissolution in aqueous solution according to

$$M^{(s)} \rightarrow M^{n+(aq)} + ze^{-} \tag{1}$$

where M is the porous anode material and $M^{n+(aq)}$ is a soluble product. It should be mentioned, however, that the same model can be applied to cathodic deposition reactions by replacing anodic by cathodic processes and vice versa.

During an electrode reaction a current passes through the electric double layer between the solid and the electrolyte. This so called Faraday current is controlled by the potential difference between the electrolyte and the solid electrode. In a more general approach, concentration gradients due to the electrochemical reaction have to be taken into account additionally. In the following, they are neglected because of the small current densities and the continuous flow of electrolyte employed in the experiment. In this case, the fundamental relationship which describes the dependence of the Faraday current density j_F on the potential difference across the solid-electrolyte interface is the Butler-Volmer equation:

$$j_F = j_0\left(\exp\frac{\alpha_a F\eta}{RT} - \exp\frac{-\alpha_c F\eta}{RT}\right) \tag{2}$$

F is the Faraday constant, R the ideal gas constant and T the temperature. j_0 (the exchange current density), α_a and α_c are constants for a given electrode reaction and electrolyte composition. The overpotential η is the difference between the potentials of the solid (η_s) and the electrolyte (η_l) with respect to the equilibrium potential of the electrode (η_0):

$$\eta = \eta_s - \eta_l - \eta_0 \tag{3}$$

For electrode reactions obeying the Butler-Volmer equation, a logarithmic plot of current versus potential yields two straight lines for high positive and negative overpotentials corresponding to the anodic and cathodic partial reaction (Fig. 2). The constants α_a and α_c in the Butler-Volmer equation can be determined from the slope of the cathodic and anodic part of the plot, respectively. The current density at which the two lines intersect is the exchange current density j_0. For a porous electrode the rate of dissolution of the electrode material per unit volume $\dot{\rho}$ can now be calculated by

$$\dot{\rho} = \frac{Mj_F S}{zF} \tag{4}$$

where a current yield of 100% has been assumed. M is the molar mass and S is the specific surface area per unit volume of the porous electrode material.

From the above it follows that it is possible to calculate the rate of dissolution of the electrode at any position if the potentials of the electrolyte and solid are known. Unfortunately the potential distribution inside the porous electrode is difficult to measure. However, it is possible to give analytical expressions for the potential distribution inside electrodes with simple geometry, if some characteristic values of the system like total current, resistivity of the electrolyte inside the pores and the constants in the Butler-Volmer equation are known. In Chapter 3.2 the underlying differential equations are derived and solved for flat and parallel electrode surfaces. In Chapter 3.3 a numerical simulation of the

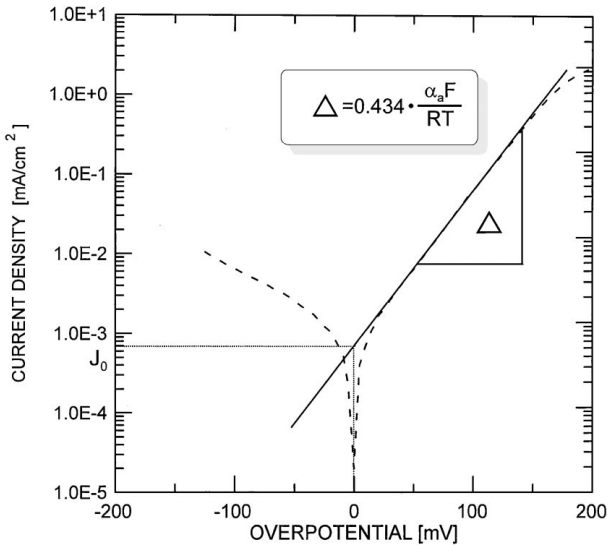

Figure 2 Current/potential curve (dashed line) and anodic Tafel-slope (full line) of a tungsten electrode in 2 mol/l NaOH (note that the current in the regime of negative overpotential is cathodic while the current flow in the regime of positive overpotential is anodic).

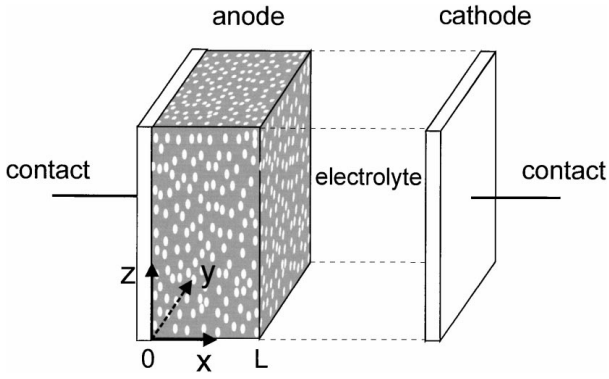

Figure 3 Basic geometry for the modelling approach.

electrochemical dissolution process is outlined—this becomes necessary if the structure of the electrode, and hence the potential distribution strongly varies during the dissolution process.

3.2. Analytical calculation of potential distribution

In the case of porous electrodes with open pore structure the resistivity of the electrolyte inside the pores leads to potential differences inside the electrode, which cause in turn a position dependent dissolution rate. The continuous or macrohomogenous model considers the electrode as a solid solution or a macrohomogenous mixture of two continuous phases (Fig. 3). The electrode has to be much larger than the particles and pores composing it. The electric double layer is small compared to pore dimensions. Pore radius is small compared to pore length. The current density in the solid phase ($\boldsymbol{j}_\mathbf{s}$) is given by Ohm's Law. For the case of constant concentration of all species in the solution the ionic current ($\boldsymbol{j}_\mathbf{l}$) is also governed by Ohm's law:

$$\boldsymbol{j}_{\mathbf{s,l}} = \frac{1}{\rho^*_{\mathrm{s,l}}} \nabla \varphi_{\mathrm{s,l}} \tag{5}$$

$\rho^*_{\mathrm{s,l}}$ is the resistivity of the porous electrode (s) and the electrolyte inside the percolating pores (l). $\varphi_{\mathrm{s,l}}$ is the potential inside the electrode and the electrolyte, and ∇ is the Nabla operator. The apparent resistivity of an electrolyte inside a porous system is higher than that of the free electrolyte due to the orientation and the topography of the conducting pores (the so called 'hydraulic tortuosity') and the local constriction of the pore cross section (the 'constriction factor') and the reduction of the cross section available for conduction [12]. As the effects of hydraulic tortuosity and constriction factor are difficult to separate experimentally, they are usually replaced by a dimensionless electric tortuosity factor $u_{\mathrm{s,l}}$ for the electrode and the electrolyte respectively. Of course, in a porous body, the ratio of cross-section available for conduction depends also on the porosity (P). Hence, the resistivity of a porous electrode and the electrolyte inside the electrode can be calculated using the following equations [13]:

$$\rho^*_\mathrm{s} = \rho_\mathrm{s} \frac{u_\mathrm{s}}{(1-P)} \quad \text{and} \quad \rho^*_\mathrm{l} = \rho_\mathrm{l} \frac{u_\mathrm{l}}{P} \tag{6}$$

ρ^*_s and ρ^*_l are the bulk resistivity of the solid (s) and the electrolyte (l), respectively. Typical values of u_l are 2–6 [12].

The condition of electroneutrality demands a balance between change of ionic current density and change of current density of the solid phase:

$$\nabla(\boldsymbol{j}_\mathbf{s} + \boldsymbol{j}_\mathbf{l}) = 0 \tag{7}$$

From Equations 5 and 7 it follows:

$$\Delta\eta = (\rho^*_\mathrm{l} + \rho^*_\mathrm{s}) \nabla \boldsymbol{j}_\mathbf{l} \tag{8}$$

Δ is the Laplace operator, η is the potential difference between the electrode and the electrolyte and differs only by an undetermined constant from the potential measured against a reference electrode. Neglecting transient response effects, the change in current density in the liquid and in the solid is proportional to the Faraday current given by the Butler-Volmer equation:

$$\nabla \boldsymbol{j}_\mathbf{l} = -\nabla \boldsymbol{j}_\mathbf{s} = S j_\mathrm{F} \tag{9}$$

For two parallel plates as electrodes (Fig. 3) it can be shown that the potential along the x axis in the central part is independent of y and z. In this case, Equations 8 and 9 yield the following differential equation:

$$\frac{\mathrm{d}^2}{\mathrm{d}x^2}\eta = S(\rho^*_\mathrm{l} + \rho^*_\mathrm{s}) j_\mathrm{F} \tag{10}$$

To solve this differential equation we can use Ohm's law (Equation 5) to get an auxiliary equation:

$$\frac{\mathrm{d}}{\mathrm{d}x}\eta = -j_\mathrm{s}\rho^*_\mathrm{s} + j_\mathrm{l}\rho^*_\mathrm{l} \tag{11}$$

The boundary conditions are that the total current in the anode is electronic at $x = 0$ ($j_\mathrm{l} = 0$ at the face away from the cathode) while the current is ionic at $x = L$ ($j_\mathrm{s} = 0$ at the face close to the cathode). Now we can distinguish two different cases:

a) *Analytical solution for large electrode polarisation* ($\eta \gg RT/\alpha F$). In the case of large electrode polarisation ($\eta \gg RT/\alpha F$) the Butler-Volmer equation (Equation 2) can be approximated by the Tafel-equation:

$$j_\mathrm{F} = j_0 \exp\left(\frac{\alpha_\mathrm{a} F}{RT}\eta\right) \tag{12}$$

After introduction of Equation 12 into the differential equation (Equation 10) the solution of the differential equation becomes:

$$\eta = \frac{RT}{\alpha_\mathrm{a} F} \ln\left[\frac{B}{2A}\left\{1+\mathrm{tg}^2\left(\left[\frac{x}{L} - x_\mathrm{min}\right]\frac{\sqrt{B}}{2}\right)\right\}\right] \tag{13}$$

L is the length of the electrode and j is the total current density in a galvanostatic experiment. A is a constant

defined as:

$$A = (\rho_l^* + \rho_s^*)L^2 S j_0 \frac{\alpha_a F}{RT} \tag{14}$$

The parameter B is determined by the following equation:

$$\text{arctg}\left(\frac{C}{\sqrt{B}}\right) + \text{arctg}\left(\frac{D}{\sqrt{B}}\right) = \frac{\sqrt{B}}{2} \tag{15}$$

with

$$C = \rho_s^* j L \frac{\alpha_a F}{RT} \quad \text{and} \quad D = \rho_l^* j L \frac{\alpha_a F}{RT} \tag{16}$$

The position of minimum overpotential $x_{\min}$ is at:

$$x_{\min} = \left(\frac{2}{\sqrt{B}}\right)\text{arctg}\left(\frac{C}{\sqrt{B}}\right) \tag{17}$$

b) *Small electrode polarisation* ($\eta \ll RT/\alpha F$). In the case of small electrode polarisation the exponential Butler-Volmer equation (Equation 2) is approximated by the first term of a Taylor series:

$$j_F = j_0 \frac{(\alpha_a + \alpha_c)F}{RT}\eta \tag{18}$$

Inserting Equation 18 in Equation 10 and solving the resulting differential equation yields

$$\eta = \frac{j}{\lambda \sinh[\lambda L]}\left\{\rho_s^* \cosh[\lambda(x - L)] + \rho_l^* \cosh[\lambda x]\right\} \tag{19}$$

with:

$$\lambda = \sqrt{j_0(\rho_s^* + \rho_l^*)S\frac{(\alpha_a + \alpha_c)}{RT}F} \tag{20}$$

Equations 13 and 19 give the position dependent overpotential inside the electrode. Inserting the calculated overpotential distribution in the Butler-Volmer equation (Equation 2) yields the Faraday current from which the position dependent weight loss can be determined using Equation 4.

3.3. Numerical simulation

The initial potential distribution allows estimation of the shape of the developed porosity gradient. However, for more precise results the change of various parameters (e.g. specific surface area) due to mass loss has to be taken into account. The mass loss depends not only on the duration of electrolysis but is also position dependent. The pore structure changes due to the dissolution process leading to position dependent porosity, specific surface area and tortuosity. All these parameters influence the potential distribution during the dissolution process. As a result the Faraday current distribution and thus the produced gradient is changed. This can be taken into account using a numerical simulation based on the same equations as the analytic solution. The numerical approach also offers the possibility to calculate potential distributions for current potential curves which cannot be described by the Butler-Volmer equation. Furthermore, electrodes of complicated shape can be modelled. In the present work, however, only a one dimensional simulation of a flat electrode was carried out. For this purpose, the electrode is divided into n elements of equal size. Each element has an electrolyte part and an electrode part representing the attributes of the pore and the solid at the specific position and time. The elements are homogenous in porosity, specific surface area and electrical resistance and all other properties. Assuming galvanostatic or potentiostatic control and using the same boundary conditions as in the analytical model, the potential development from one element to the next can be calculated regarding the elements as a network of resistances and calculating the Faraday current for each element separately using Equations 2 and 6. A schematic plot of the numerical model is sketched in Fig. 4. The algorithm varies the potential (galvanostatic case) or the current (potentiostatic case) until the boundary conditions are fulfilled. It is now possible to include the time dependence of the electrode and electrolyte properties by recalculating the potential distribution after a sufficiently small time interval during the total duration of the experiment.

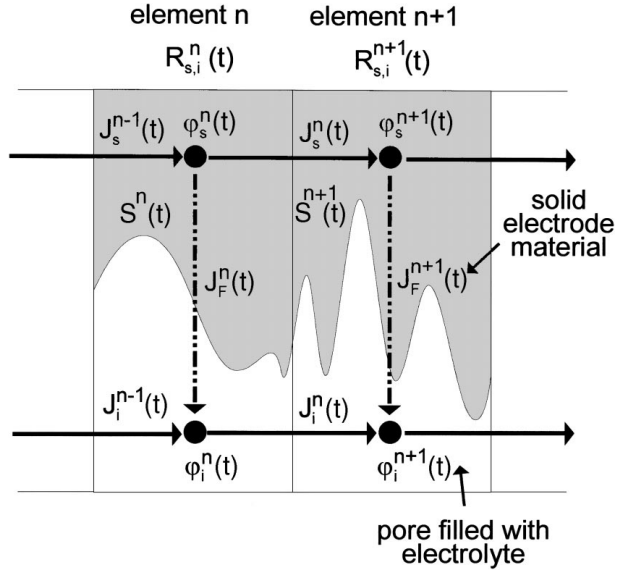

Figure 4 Principle of the finite element simulation of the potential distribution ($R^n_{s,1}(t)$ is the time dependent resistance of the electrode (s) and the electrolyte (e) in the n-th element).

4. Experimental procedure

The processing method described here was applied to the fabrication of W/Cu gradient materials. This system has a number of advantages: The anodic dissolution of W obeys the Butler-Volmer equation in a very wide potential range (cf. Fig. 2), and it has a current yield of 100% (no side reactions are taking place). Additionally, porous W can be infiltrated with a variety of metals with low melting points (e.g. Cu, Ag, . . .).

Tungsten preforms with an open porosity between 16 and 42% and about $30 \times 30 \times 6$ mm^3 size were used

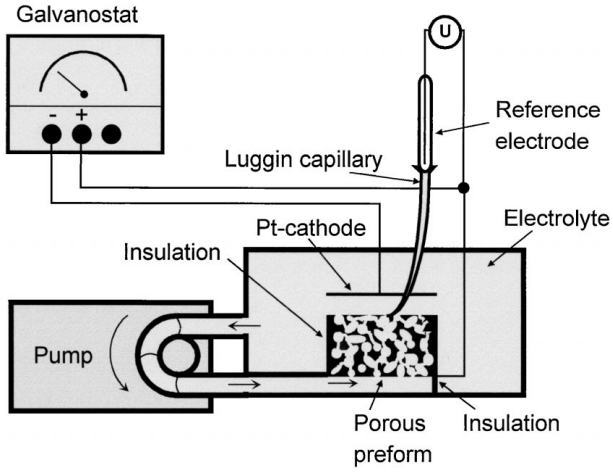

Figure 5 Experimental set-up for electrochemical gradation.

as starting material. They were produced by partially sintering tungsten powders of either 4 or 10 μm average grain size containing about 1% nickel (Tridelta AG, Germany). The preforms were graded in an electrochemical cell (see Fig. 5). For this purpose the preforms were weighed, fixed in a dense insulating elastomer and connected to the anode of a galvanostat through of a platinum wire. This prevents penetration of the electric field from the side into the sample. A platinum plate with the same area as the anode was used as a cathode and mounted parallel to the anode at a distance of about 10 mm. Both electrodes were placed in a container filled with commercial grade NaOH electrolyte in different concentrations. A pump connected to the bottom of the anode provided a continuous flow of electrolyte through the porous tungsten maintaining the electrolyte concentration inside the pore network almost constant and removing the reaction products. A reference electrode was placed as near as possible to the front of the anode by means of a Luggin capillary. This allowed recording the potential during the experiment.

For the gradation of tungsten the anodic dissolution reaction of tungsten in alkaline solution has been used. The reaction consists of the oxidation of tungsten to tungsten trioxide and subsequent dissolution of the tungsten trioxide in the alkaline electrolyte. The formation of WO_3 is a multistep reaction consisting of fast formation of WO_2, which is oxidised in a rate controlling step to solid WO_3:

fast

$$W^{(s)} + 4OH^- \rightarrow WO_2^{(s)} + 2H_2O + 4e^- \quad (21)$$

rate determining

$$WO_2^{(s)} + OH^- \rightarrow WO_3^{(s)} + H^+ + 2e^- \quad (22)$$

The formed WO_3 dissolves in the NaOH solution according to

$$WO_3^{(s)} + 2OH^- \rightarrow WO_4^{2-(aq)} + H_2O \quad (23)$$

The reactions (21)–(23) are quantitative, the current yield is therefore 100%.

TABLE I Experimental conditions for electrochemical gradation

Sample	A	B	C	D	E
Porosity (%)	25	25	42	42	16
NaOH concentration (mol/l)	2	2	2	1	1
Current density (mA/cm^2)	5.5	12.2	5.5	5.5	5.6
Duration of anodisation (h)	194	88	194	194	235
Current yield (%)	100	100	100	100	100

All experiments were carried out under galvanostatic conditions. In different experiments, the current, electrolyte concentration and starting porosity were varied (see Table I). The total amount of charge passed through the electrode was kept constant. The conductivity of the electrolyte was measured at the beginning and the end of the experiment. This was necessary because the resistivity of the electrolyte is increasing during the dissolution process due to the consumption of sodium hydroxide (Equation 23). The total amount of charge passed through the electrode was kept constant. After electrolysis the samples were flushed several times with water and dried in a drying chamber in order to remove the remaining electrolyte. Remaining reaction products on the surface of the preforms (e.g. lower tungsten oxides) were reduced in a hydrogen atmosphere at 850 °C for 20 min in order to improve the wetting behaviour of the preforms with copper. An additional hold at 1050 °C for 20 min was used to achieve isothermal conditions in the samples. Then the samples were infiltrated with liquid copper at 1250 °C for 1/2 h in a hydrogen atmosphere. In some cases it was noticed that the combination of a longer reduction time and additional pressure during the infiltration process improves the infiltration behaviour.

For the evaluation of the position dependent composition, the samples were cut parallel to the gradient with a diamond cutting wheel. Then the sections were ground and polished. An optical microscope with an image analysing system was employed for the quantitative determination of the phase content (QUANTIMET, Leica Germany). Due to the good optical contrast between the red copper phase and the blue tungsten phase, the reproducibility of the measurement is high. Error bars in the plots arise mainly from inhomogeneities of the microstructure and from sample preparation. A number of measurements perpendicular to the gradient were carried out to reduce the error. The mean relative variance is about 2%. A standard Vickers indenter using a load of 49.03 N and a holding time of 10 seconds was used for hardness testing. Again a number of measurements perpendicular to the gradient were carried out to reduce the error. The local specific surface area of samples with different microstructures was determined using a stereological method.

5. Results and discussion

5.1. Electrochemical parameters

In order to predict the porosity gradient developed in the tungsten electrodes, it was first necessary to determine the parameters required for electrochemical modelling, that is the constants in the Butler-Volmer

equation and the resistivity of the electrolyte in the porous system. In order to determine the constants in the Butler-Volmer equation, a polished flat tungsten electrode of known area was held at different potentials and the current was recorded. The resulting plot of current versus potential is shown in Fig. 2. The logarithmic plot of current versus potential is nearly linear for high positive and negative overpotential $|\eta| > 20$ mV. From the anodic part of the plot (positive overpotential) the parameters j_0 and α_a were extracted as $j_0 = (7 \pm 0.5) \times 10^{-4}$ A/m^2 and $\alpha_a = 1.17 \pm 0.05$.

In order to determine the resistivity of the electrolyte in the porous system using Equation 6, the porosity of the electrode, bulk electrolyte resistivity and the electric tortuosity factor are necessary. The first two parameters are easily accessible by density and conductometric measurements. The electric tortuosity factor of the electrolyte u_l was determined by placing a porous tungsten sample in the middle between two flat graphite electrodes in a container filled with sodium hydroxide. If a DC current was passed through the electrolyte a potential difference across the tungsten sample occurred, which was measured using two Luggin capillaries. The electric tortuosity factor determined from the potential drop was 6.7 ± 0.5 for the 25% porous tungsten (sample C and D) and 2.25 ± 0.5 for the 42% porous tungsten (sample A and B). Due to the low resistivity of the electrode material used ($\rho_W = 5.4 \times 10^{-8}$ Ωm) compared to the electrolyte resistivity ($\rho_{NaOH} = 3 - 6 \times 10^{-2}$ Ωm) the potential of the porous electrode is nearly constant and the effect of the tortuosity factor for the solid on the gradation process is negligible. It was therefore not determined and set equal to the tortuosity factor of the electrolyte.

5.2. Graded materials

Fig. 6 shows a representative microstructure of a graded W/Cu composite that was produced by electrochemical gradation of W and subsequent Cu infiltration (Sample E). A one dimensional gradient in tungsten content (dark areas) from the side distant to the cathode to the side near to the cathode is observed. The tungsten content varies from 20 to 80 vol % within a distance of about 1.5 mm. The gradient is continuous and accompanied by an increase in the size of copper ligaments (light area). Only at the former outer surface of the tungsten preform on the right side of the micrograph a sudden change from about 80 to 100% copper content is observed.

Fig. 7 shows the volumetric tungsten content as a function of position for sample B. The dashed line is the result of the analytical model for large overpotential which uses the potential distribution at the beginning of the experiment to calculate the developed gradient. Although the analytical model fits the data reasonably well, a numerical calculation including time dependent effects was carried out. For precise modelling, knowledge of the changes of the porous electrode during the gradation process parameters is crucial. Therefore the change of specific surface area of the porous electrode as a function of relative density was determined by image analysis of electrochemically graded samples [14]. The results of the specific surface area measurements are displayed in the diagram of specific surface area versus relative density, Fig. 8. It can be seen that with decreasing relative density the specific surface area first increases and then decreases after reaching a maximum value at 50–60 vol % tungsten content. The initial increase in specific surface area with decrease in relative

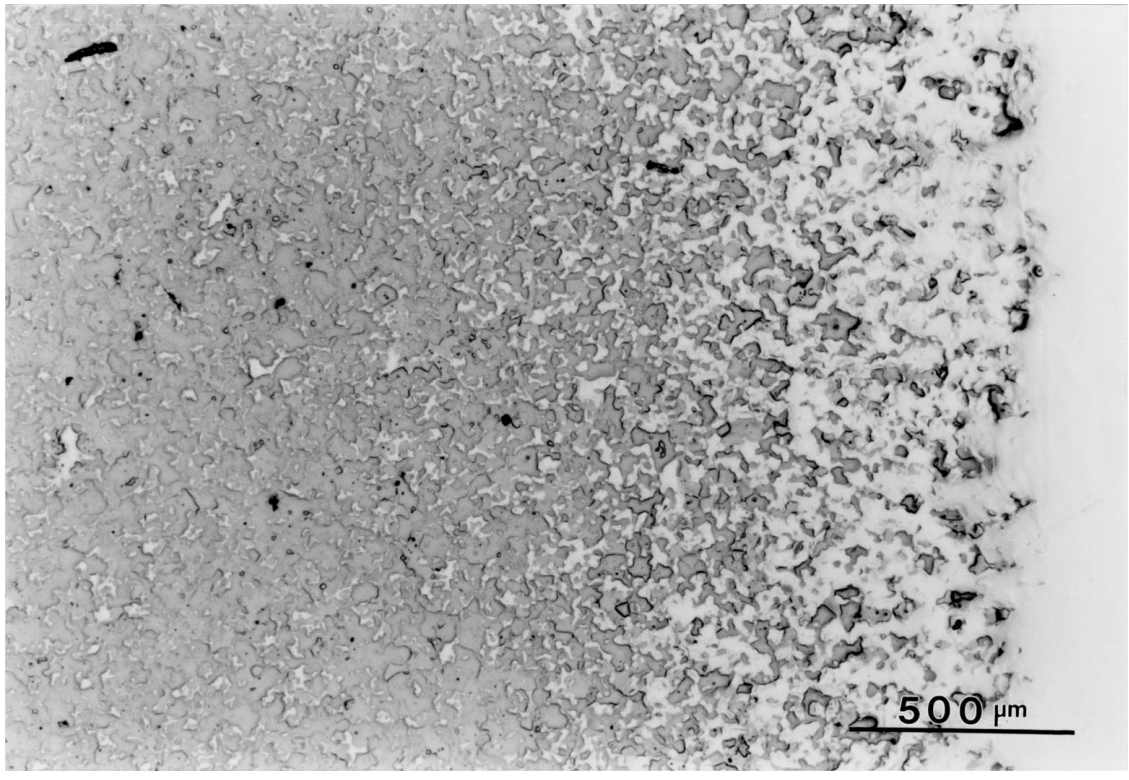

Figure 6 Micrograph of sample E showing gradation from the dark tungsten phase to the light copper phase.

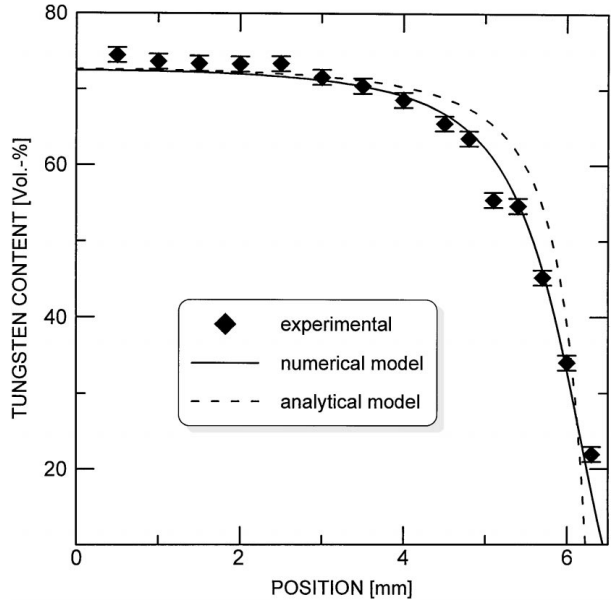

Figure 7 Comparison of the predicted and observed gradation profiles for sample B.

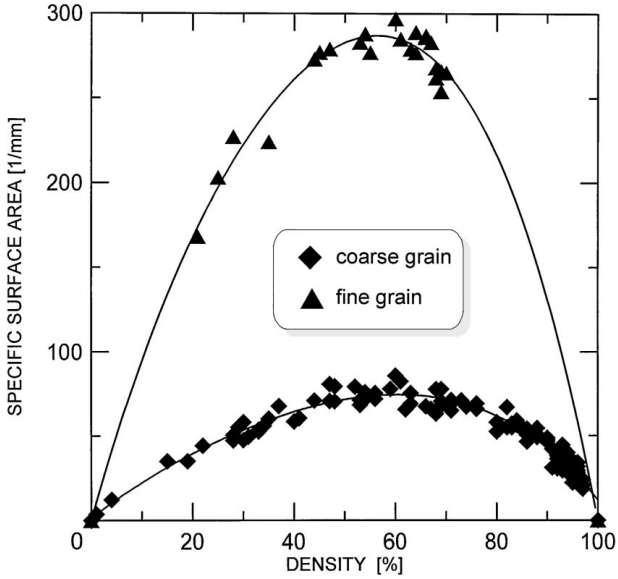

Figure 8 The dependence of specific surface area on the density and grain size of tungsten.

density is explained by an increase in average pore size due to the dissolution process. At higher porosity levels, the growing pores start to coalesce leading to a decrease of surface area. The absolute values of the specific surface area depends of course on the microstructure of the sample. The fine grained porous W shows a specific surface area about 4 times higher than the coarse grained material at all porosity levels.

As the porosity and surface area of the electrode changes during the dissolution process, the overpotential distribution will also change. In Fig. 9, the overpotential distribution calculated using the numerical approach is displayed for sample B. It can be seen that the gradient in overpotential at the beginning of the electrochemical gradation experiment is steeper than at the end of the experiment. This can be explained qualitatively by the opening of pores on the right side of the figure,

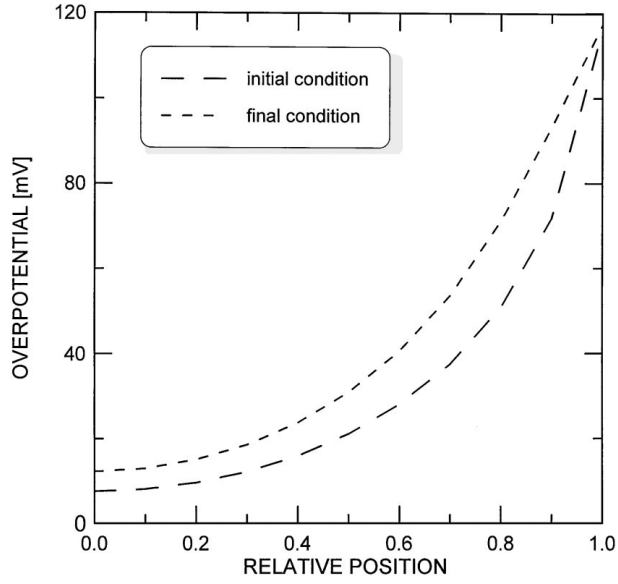

Figure 9 Distribution of overpotential vs. relative position.

which makes the inner part of the electrode more accessible to the dissolution process. The full line in Fig. 7 shows the result of the numerical model including the time-dependent effects. It can be clearly seen that the numerical model fits the experimental data better than the analytical approach.

As mentioned earlier, the gradation profile can be varied by selecting different experimental conditions. Fig. 10 shows the results of the gradation with varying experimental parameters. The plots show the volumetric tungsten content and the hardness values versus the sample thickness. As could be expected, the gradient in composition is reflected in a change of Vickers hardness. Comparing the plots, several influences of the experimental parameters on the shape of the gradient are apparent. In plots of sample A and B it can be seen that increasing the total current (B) and keeping the other experimental parameters constant yields higher potential differences and a steeper gradient. Increasing the resistivity of the electrolyte by decreasing the concentration of NaOH and keeping the other parameters constant also leads to a steeper gradient (compare sample C and D). This can also be explained by an increase in potential difference across the porous electrode: at the same current density the potential drop will be higher in an electrolyte with low conductivity. The effective conductivity of the electrolyte in the porous system is also decreasing with porosity: therefore preforms with lower initial porosity graded under the same experimental conditions also show steeper gradients (compare sample B and D).

It was not possible to produce graded preforms with a smooth gradient of porosity up to 100 vol %. The highest possible porosity value is given by the point at which the microstructural elements of the preform are no longer percolating. For equiaxed grains the percolation limit is about 18 vol % [15]. This coincides with the lowest relative density observed in the graded tungsten preforms which is 18–20 vol %. The lower limit of porosity of the graded preforms is dictated by the requirement that the major part of the porosity of the

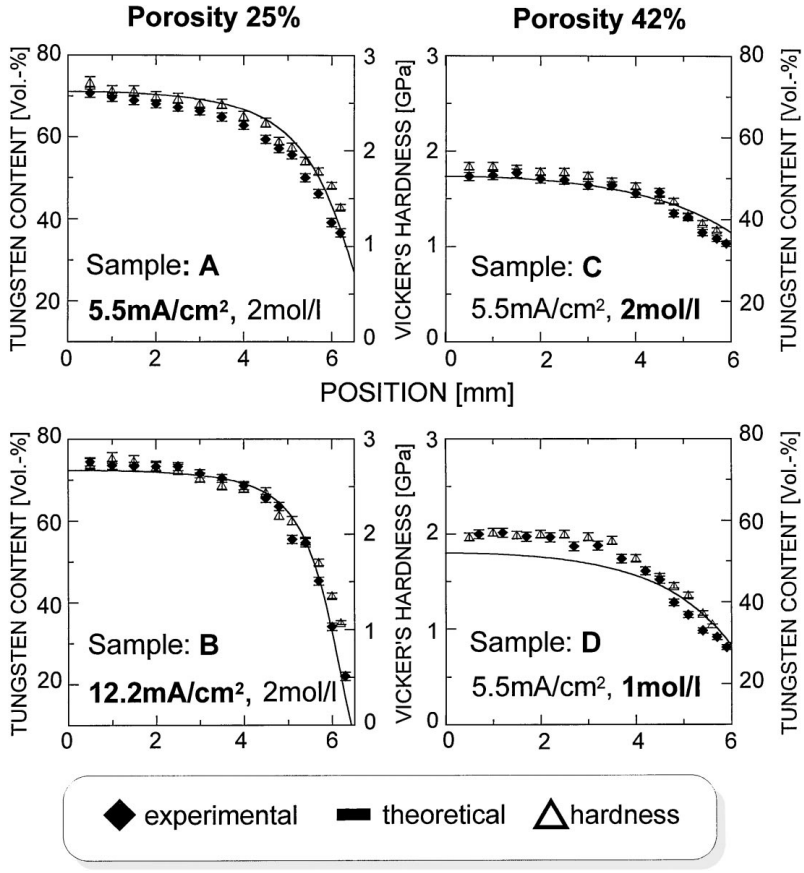

Figure 10 Gradation results for different experimental conditions.

preform must be open. With the tungsten preforms used in this work, the lowest porosity achieved was about 16 vol %, but using special techniques like capsule-free hot isostatic pressing, preforms with less than 5% open and no closed porosity can be produced [9].

The full lines in Fig. 10 are the results of the numerical model. It can be seen that the model predicts the shape of the gradient well. Nevertheless, slight differences between the predicted and actual gradients are observed. Apart from experimental errors in the determination of the volume content of the different phases, the dependence of the tortuosity factor on the porosity could be responsible for the remaining differences. During the experiment the porosity and also the tortuosity factor becomes position dependent. As no detailed data on the dependence of tortuosity on porosity were available, it was assumed to be constant throughout the experiment in the numerical simulation. This may account for the remaining differences between the predicted and observed gradient. Of course, the numerical model not only simulates the evolution of the porosity gradient, but also of other quantities like overpotential. There were differences in the order of 140 mV between the overpotential measured at the front surface of the porous electrode and the calculated values. These differences could be explained in the following way: For the numerical simulation the stereologically determined specific surface area was used—this is not identical to the electrochemically active specific surface in a porous electrode, which is defined as the surface area of the electrical double layer. Additionally, the porosity contained in the porous anode was open, but nevertheless there was a certain amount of pores with dead ends. Inside these, the exchange of chemically active species due to liquid flow is restricted. NaOH is consumed when tungsten is dissolved anodically (see Equation 23). Therefore, the concentration of sodium hydroxide in pores with insufficient flow of liquid would decrease and the surface area in this region would become inactive due to oxide surface layers of increasing thickness. In such a case the apparent electrochemically active specific surface area would be smaller than the optically determined one. Measurements of the electrochemically active specific surface based on a current jump proposed by Rousar *et al.* [13] indeed indicate that the electro-chemically active surface area is about a factor of ten smaller than the specific surface area determined by microscopy. Such a difference can account for most of the deviation in the measured and observed overpotential. Despite the difficulties of predicting the absolute value of the overpotential due to the above mentioned effects, the model proposed here will be able to predict the gradients in a reliable way in the case of high overpotential. Then in a galvanostatic experiment the overpotential gradient inside the porous electrode (which governs the produced gradients) does not depend on the surface area, whereas the absolute value of overpotential does.

Electrochemical gradation offers a number of advantages over other methods. It is possible to build continuous gradients in a single electrochemical step. The slope of the gradient can be controlled in a simple way by varying experimental parameters. The only limitation that electro-chemical gradation sets on the gradient is

that its basic shape is always governed by Equations 13 or 19. Gradients of different symmetry and complicated shape can be realised by using anodes and cathodes with appropriate geometry. For example, two-dimensional gradients can be produced if a non-planar counter electrode is used. Employing a cylindrical porous anode surrounded by a cylindrical electrode leads to a gradient material with radial symmetry.

In the present work, tungsten has been chosen as an electrode material because its anodic dissolution in NaOH is quantitative and current-potential curves are well reproducible. It is expected that the method can also be applied to other starting materials. However, in many cases the electrochemical reactions taking place are more complex due to side reactions, passivation effects etc. One such example is the anodic oxidation of carbon mentioned earlier where many different oxidation products (carbon dioxide, carbon monoxide, oxygen, polycarboxylic acids and so on) may be formed simultaneously. First experiments for this system indicate that even in this case suitable experimental conditions for the gradation can be found with the model proposed here, although the precise shape will not be predicted. Despite the fact that the electrochemical gradation process takes several days for thick samples, it appears suitable for mass production of FGM's, because the cost of the gradation step is low and large components can be produced by scaling up the electrochemical cell. In the case of W/Cu composites, the gradation step can be easily integrated in an already existing industrial process consisting of producing ungraded porous tungsten preforms and infiltration.

6. Conclusions

The electrochemical gradation of porous preforms is a versatile method to produce a wide range of metal/metal or ceramic/metal gradient materials. It has been demonstrated that dense W/Cu FGM's with a well defined and continuous gradient can be produced by electrochemical treatment of porous tungsten preforms and subsequent infiltration with molten copper. The shape of the gradient can be varied by adjusting experimental parameters like current density, electrolyte resistivity, duration of electrolysis, electrode geometry or porosity. A macroscopic model of the electrode kinetics based on the Butler-Volmer equation affords a predictive capacity for the accessible gradation profiles. An analytical solution of the underlying differential equations for the initial potential distribution is possible and allows a qualitative prediction of the gradient. A precise model of the gradation process taking into account microstructural changes of the porous electrode during the dissolution process leads to full agreement of the observed and calculated gradation profile. The basic shape of the produced gradients is always governed by the transcendental functions (Equation 13) or (Equation 19). Despite the limitation concerning the shape of the produced gradation profiles, the presented method appears attractive from the point of view of industrial application, because it allows production of fully dense gradient materials at moderate cost.

Acknowledgements

This work was supported by the German Research Society (DFG) under contract number Ne599/1-2. We also thank Tridelta AG for kindly supplying the tungsten preforms and Prof. Dr. B. Kastening for assistance in developing the model of the electrochemical gradation process. We are indebted to U. Hahn and Prof. Dr. D. Stoyan for determining the specific surface of the graded W samples.

References

1. A. MORTENSEN and S. SURESH, *International Materials Reviews* **40** (1995) 239.
2. A. NEUBRAND and J. RÖDEL, *Z. Metallkd.* **88**(5) (1997) 357.
3. D. DELFOSSE and B. ILSCHNER, *Mat.-wiss. u. Werkstofftechnik* **23** (1992) 235.
4. B. R. MARPLE and J. BOULANGER, *J. Amer. Ceram. Soc.* **77** (1994) 2747.
5. H. MORI, Y. SAKURAI, M. NAKAMURA and S. TOYAMA, in "Proceedings of the 3rd International Symposium on Structural and Functionally Gradient Materials," edited by B. Ilschner and N. Cherradi (Presses Polytechniques et Universitaires Romandes, Lausanne, 1995) p. 173.
6. A. SALITO and G. BARBEZAT, in "Proceedings of the 3rd International Symposium on Structural and Functionally Gradient Materials," edited by B. Ilschner and N. Cherradi (Presses Polytechniques et Universitaires Romandes, Lausanne, 1995) p. 123.
7. M. SEKI, M. AKIBA, M. ARAKI, K. YOKOYAMA, M. DAIRAKU, T. HORIE, K. FUKAYA, M. OGAWA and H. ISE, *Fusion Engineering and Design* **15** (1990) 59.
8. Y. ITOH, M. TAKAHASHI and H. TAKANO, *ibid.* **31** (1996) 279.
9. M. TAKAHASHI, Y. ITOH, M. MIYAZAKI, H. TAKANO and T. OKUHATA, in "Proceedings of the 13th International Plansee Seminar," edited by H. Bildstein and R. Eck (Metallwerk Plansee, Reutte, 1993) p. 17.
10. M. TAKAHASHI, Y. ITOH, European Patent No. 446934 B1 (1998) edited by I. Shiota and M. Y. Migamoto (Elsevier, Amsterdam, 1997) p. 167.
11. M. JOENSSON, U. BIRTH and B. KIEBACK, in "Proceedings of the 4th International Symposium on FGM 96," in press.
12. F. A. L. DULLIEN, "Porous Media; Fluid Transport and Pore Structure," ed. (Academic Press, Inc., California, 1992).
13. I. ROUSAR, K. MICKA and A. KIMLA, in "Electrochemical Engineering, Chemical Engineering Monographs (21B)" (Elsevier, Amsterdam, 1986).
14. U. HAHN and D. STOYAN, in "Proceedings of the International Conference on the Quantitative Description of Materials Microstructure," edited by L. Wojnar and K. Rozniatowski (Warsaw 1997).
15. W. POMPE, private communication.

Received 26 August 1997
and accepted 20 July 1999